3148 *Biochemistry* **2010,** *49,* 3148–3155
DOI: 10.1021/bi902189s

BIOCHEMISTRY
including biophysical chemistry & molecular biology
Article

Recognition of siRNA Asymmetry by TAR RNA Binding Protein†

Joseph A. Gredell, Michael J. Dittmer, Ming Wu, Christina Chan, and S. Patrick Walton*

Department of Chemical Engineering and Materials Science, Michigan State University, East Lansing, Michigan 48824-1226

Received December 21, 2009; Revised Manuscript Received February 24, 2010

ABSTRACT: The recognition of small interfering RNAs (siRNAs) by the RNA-induced silencing complex (RISC) and its precursor, the RISC loading complex (RLC), is a key step in the RNA interference pathway that controls the subsequent sequence-specific mRNA degradation. In *Drosophila*, selection of the guide strand has been shown to be mediated by RLC protein R2D2, which senses the relative hybridization stability between the two ends of the siRNA. A protein with similar function has yet to be conclusively identified in humans. We show here that human TAR RNA binding protein (TRBP) alone can bind siRNAs in vitro and sense their asymmetry. We also show that TRBP can bind 21-nucleotide single-stranded RNAs, though with far lower affinity than for double-stranded siRNA, and that TRBP cross-links preferentially to the 3′-ends of the guide strands of siRNAs. This suggests that TRBP binding depends both on the sequences of the siRNA strands and on the relative hybridization stability of the ends of the duplex. Together, these results demonstrate the importance of the siRNA−TRBP interaction in the selection of the siRNA guide strand in RNAi.

RNA interference (RNAi) is a means of specifically silencing the expression of a target gene (*1*, *2*). The pathway can be initiated by long double-stranded RNAs (dsRNAs)[1] or pre-microRNAs (pre-miRNAs) processed by the ribonuclease III family enzyme Dicer into 21−27 nucleotide (nt), double-stranded small interfering RNAs (siRNAs) or miRNAs with 5′-phosphates and 3′-dinucleotide overhangs (*3*). Alternatively, siRNAs with the proper structure can be added directly to cells for initiation of the pathway (*4*, *5*). In both cases, silencing is initiated through the RNA-induced silencing complex (RISC) and its predecessor, the RISC loading complex (RLC) (*6*, *7*). The RLC is minimally comprised of Dicer, the TAR RNA binding protein (TRBP), and Argonaute 2 (Ago2), although several other proteins have been shown to associate with the RLC and RISC in vivo (*8*−*14*). Ago2 is the catalytic component of RISC responsible for degradation of the complementary passenger siRNA strand for generation of active RISC and cleavage of the target mRNA for silencing (*15*−*20*). Though it makes no enzymatic contribution to siRNA-initiated RNAi, Dicer has been shown to contribute to siRNA processing by coupling dsRNA processing to guide strand loading onto Ago2 (*21*−*23*), a role supported by the structure of the RLC in vitro (*24*). While the same structural studies suggested that TRBP can stabilize the RLC (*24*), a precise functional contribution of TRBP to siRNA processing has yet to be confirmed.

TRBP was first identified by its ability to bind the TAR RNA structure present in human immunodeficiency virus (HIV-1) transcripts (*25*). Later, it was shown that TRBP can inhibit protein kinase R (PKR), an important contributor to the innate response to viral infection (*26*). Most recently, it was found that TRBP interacts directly with Dicer, as well as the activator of PKR (PACT), through the Medipal domain present at the C-terminus of TRBP (*27*), and that the interaction is not mediated solely by dsRNA (*9*, *28*). A similar interaction is detected in *Drosophila*, where Dicer-2 associates with dsRNA binding protein (dsRBP) R2D2 (*29*). Together, the Dicer-2−R2D2 complex senses the relative thermodynamic asymmetry within an siRNA (*7*). R2D2 binds to the more stable (dsRNA-like) end, leaving Dicer-2 to bind the opposite end. Furthermore, binding is enhanced by the presence of a 5′-phosphate on the passenger strand; hydroxyl groups, such as those present during chemical siRNA synthesis, inhibit binding (*7*). As a result of the asymmetric binding, the guide strand is preferentially loaded into active RISC, and the passenger strand is degraded (*17*, *20*).

Extensive data have shown that human RISC senses asymmetry between the ends of the siRNA or miRNA−miRNA* duplexes, leading to the preferential incorporation of one strand as the guide strand of the active RISC (*6*, *13*, *30*, *31*). This has been accomplished with crude cell extracts and immunopurified proteins (*6*, *13*), and more recently using only recombinant Dicer, TRBP, and Ago2 in a 1:1:1 stoichiometry (*10*). Asymmetric strand loading by human RISC is also demonstrated in analyses of large siRNA or miRNA data sets (*30*, *31*) and is currently the cornerstone for predicting siRNA efficacy (*32*, *33*). However, unlike in *Drosophila*, no studies using human cells or proteins have conclusively shown how siRNA asymmetry is detected. Since Ago2 alone cannot bind and select the siRNA guide strand (*19*), it suggests that its partners in the RLC, Dicer and/or TRBP, contribute to initial siRNA loading, even though other

†Financial support for this work was provided in part by Michigan State University, the National Science Foundation (Grant 0425821), and the National Institutes of Health (Grants CA126136, GM079688, and RR024439).

*To whom correspondence should be addressed: Applied Biomolecular Engineering Laboratory of the Cellular and Biomolecular Laboratory, Department of Chemical Engineering and Materials Science, Michigan State University, 3249 Engineering Building, East Lansing, MI 48824-1226. Telephone: (517) 432-8733. Fax: (517) 432-1105. E-mail: spwalton@egr.msu.edu.

[1]Abbreviations: AS, antisense strand; dsRNA, double-stranded RNA; dsRBD, dsRNA binding domain; dsRBP, dsRNA binding protein; miRNA, microRNA; nt, nucleotide; RISC, RNA-induced silencing complex; RLC, RISC loading complex; siRNA, small interfering RNA; SS, sense strand; TRBP, TAR RNA binding protein.

 Published on Web 02/25/2010

factors such as RNA helicase A (RHA) or PACT may also have an effect in vivo (*11*, *12*, *14*).

We were interested in characterizing the binding of siRNAs by recombinant TRBP in vitro to determine whether TRBP could sense asymmetry in siRNAs. Our results show that TRBP binds siRNAs and not the analogous siDNAs or siDNA−RNA hybrids. Furthermore, we demonstrate that TRBP alone can sense the asymmetry of an siRNA duplex, thus establishing a key functional role for TRBP in the human RNAi pathway. Additionally, TRBP bound 21 nt ssRNAs in a manner that reflected the asymmetry detected in their corresponding siRNA duplex, providing an indication that TRBP−RNA binding may also be sequence-dependent.

MATERIALS AND METHODS

Protein Expression and Purification. Plasmids encoding TRBP as a fusion product with maltose binding protein (MBP−TRBP) and MBP alone were kindly provided by A. Gatignol and expressed essentially as described previously (*27*). Briefly, plasmids were transformed into Rosetta2(DE3) competent cells (Novagen). An overnight culture from a single colony was diluted 1:50 (v/v) and grown for 3−4 h at 37 °C, or until the A_{600} reached 0.6−1.0, and then induced with 0.3 mM IPTG. After being expressed for 2 h at 37 °C, cells were pelleted (4000 rpm for 10 min), resuspended in column buffer (20 mM Tris-HCl, 200 mM NaCl, and 1 mM EDTA), lysed via sonication, and then clarified by high-speed centrifugation (15000 rpm for 25 min). The supernatant was purified with an AKTA FPLC system (GE Healthcare). MBP−TRBP and MBP were eluted from a MBPTrap column (GE Healthcare) with 5 column volumes of elution buffer (20 mM Tris-HCl, 200 mM NaCl, 1 mM EDTA, and 10 mM maltose) and stored in elution buffer at −80 °C until they were used.

Protein concentrations were measured with a Bradford assay (Bio-Rad) or bicinchoninic acid (BCA) assay (Pierce, Thermo Scientific). Products were assessed by separating approximately equal amounts of protein per lane on denaturing linear 4 to 20% Tris-HCl gels. Total protein was visualized by staining with Gel Code Blue (Pierce, Thermo Scientific), with a final estimated purity of >90% determined by band quantification, and specific proteins were detected via Western blotting. For the Western blot, the separated proteins were transferred to nitrocellulose membranes and then incubated overnight at 4 °C with the appropriate antibodies [MBP (New England Biolabs) and TRBP (Abnova)]. Blots were washed with TBS-Tween, incubated for an additional 1 h with HRP-linked secondary antibody (Pierce, Thermo Scientific), and developed using the SuperSignal West Femto Maximum Sensitivity Substrate kit (Pierce, Thermo Scientific). Images were obtained on a Bio-Rad ChemiDoc XRS imager using Quantity One.

Nucleic Acids. The nucleic acid sequences are listed in Tables 1−5 of the Supporting Information. The pp-luc and sod1 sequences are identical to siRNA '1' and siRNA 'a' from ref *7* and had also been used previously by the Zamore group (*34*). DNA oligonucleotides were purchased from Integrated DNA Technologies. Chemically synthesized RNAs were purchased from Dharmacon as either ready-to-use siRNAs or ssRNAs. HIV-1 TAR RNA was prepared by in vitro transcription from a plasmid kindly provided by K.-T. Jeang. Briefly, 1 μg of linearized plasmid DNA was transcribed with the Megashortscript Kit (Ambion) following the manufacturer's instructions. Transcripts were resolved in 8 M urea/10% polyacrylamide gels, visualized by UV shadowing, and eluted from gel slices by being crushed and soaked in TE buffer (10 mM Tris and 1 mM EDTA) for 10 min at 75 °C. RNA was then concentrated by ethanol precipitation, washed with 70% ethanol, and quantitated spectrophotometrically (NanoDrop). To remove the 5′-triphosphate, RNAs were treated with calf intestinal phosphatase (New England Biolabs). Treated RNAs were purified first by phenol/chloroform extraction, then precipitated with ethanol, gel purified (as above), and concentrated. The concentration of the product containing the 5′-OH group was again measured prior to end labeling with [γ-^{32}P]ATP (see below).

Duplex Preparation and End Labeling. For Figure 2, oligonucleotides were hybridized by mixing equal amounts of both top and bottom strands in 1× STE buffer (10 mM Tris, 100 mM NaCl, and 1 mM EDTA) and then heated to 90 °C for 3 min, followed by incubation at 37 °C for 60 min. Products were verified on native TBE gels stained with SYBR Gold (Invitrogen). Duplexes for Figure 2 and ssRNAs (Figure 6) (3 pmol) were directly 5′-radiolabeled with 10 pmol of [γ-^{32}P]ATP using T4 polynucleotide kinase (New England Biolabs); unincorporated label was removed using G-25 Sephadex columns (Roche Applied Science). TAR RNA (3 pmol) was similarly labeled following CIP treatment.

For the remaining figures in which strands were alternately hot and cold labeled, individual single strands (3 pmol) were labeled as described above (10 pmol of ATP) in 25 μL reaction mixtures, where nonisotopic ATP was used for cold labeling. The 5′-O-methyl-modified strands were not end labeled. The two strands comprising the siRNA duplex were then mixed (50 μL); 5.56 μL of 10× STE was added for a final concentration of 1.0× STE, and samples were heated to 90 °C for 3 min and then cooled to 37 °C for 60 min. Unincorporated label was then removed from the annealed siRNA using the Sephadex columns. Final products were verified on native TBE gels.

Native Gel Shift Assay. TRBP binding was assessed by gel shift assays using radiolabeled oligonucleotides present at limiting concentrations relative to protein concentrations. Binding reaction mixtures (10 μL) were prepared with ∼1−3 × 10^4 cpm of nucleic acid and 350 nM MBP−TRBP (unless noted otherwise) in elution buffer supplemented with 20 mM HEPES, 40 mM KCl, 1.5 mM $MgCl_2$, 0.1% Nonidet P40, and 10 units of SUPERase-In (Ambion). Samples were incubated at room temperature for 30 min and mixed with 2 μL of 5× nucleic acid sample loading buffer (Bio-Rad), and 10 μL was loaded onto a prerun native TBE gel. Minigels in which the top half of the gel was 4% (37:1 acrylamide:bisacrylamide) and the bottom half was a gradient between 4 and 20% were prepared. Gels were run at 150 V for ∼40 min, dried on filter paper under vacuum at 80 °C for 50 min, exposed to a storage phosphor screen overnight (∼12−16 h), and then imaged on a Storm 860 imager (GE Healthcare). Relative signal intensities were quantified using Quantity One and normalized within a single lane. Native gels for loading control were similarly prepared but with the volume of MBP−TRBP replaced with an equal volume of elution buffer.

UV Cross-Linking, Denaturing Gel Shift Assay. Cross-linking of MBP−TRBP to nucleic acids was assessed as in the native gel shift assay except that after the initial 30 min binding, the samples were subsequently exposed to 312 nm UV light (Fisher Scientific Electrophoresis Systems Transilluminator) for 10 min while on an ice-cold aluminum block (4 °C). To minimize

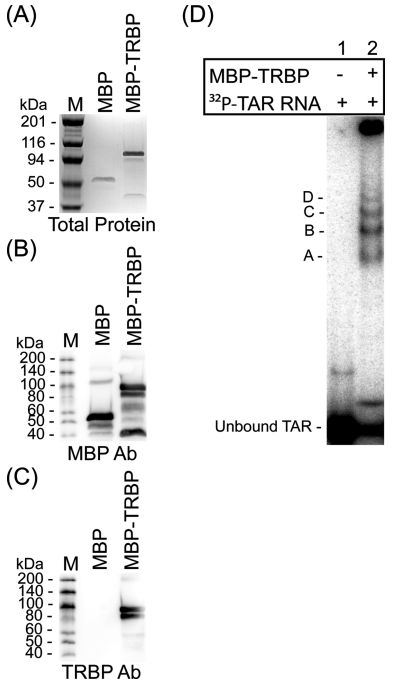

FIGURE 1: Characterization of recombinant TAR RNA binding protein (TRBP). Recombinant TRBP was prepared as a fusion product with maltose binding protein (MBP) as described in Materials and Methods. (A) Purified MBP or MBP−TRBP proteins were resolved via SDS−PAGE and visualized by being stained with Gel Code Blue. (B and C) Western blots of gels shown in panel A were performed with antibodies specific for (B) MBP or (C) TRBP. (D) Gel mobility shift analysis of MBP−TRBP with ^{32}P-labeled TAR RNA achieved via incubation of 1000 nM protein with a limiting amount of TAR RNA (10^4 cpm, < 1.0 nM) and resolution of protein−RNA complexes by native PAGE. Four distinct complexes were visible (bands A−D). Lane M contained protein size markers (kilodaltons).

nonspecific cross-linking, we covered the samples with a Petri dish to block shorter wavelengths. Samples were then mixed with 5 μL of 3× SDS sample buffer (New England Biolabs), boiled at 95 °C for 3 min, and collected by brief centrifugation, and 12 μL of the sample was loaded onto a prerun nonlinear denaturing 4 to 20% Tris-HCl gel. Gels were run, dried, imaged, and analyzed as described above. On the basis of a comparison of native binding on native gels and cross-linked sequences run on denaturing gels, we estimate roughly 5−10% cross-linking efficiency (in Figure 4, compare panels A and B). Statistical analyses are reported as *p* values from an unpaired, two-tailed Student's *t* test assuming unequal variance performed using Microsoft Excel.

RESULTS

Production and Characterization of Recombinant MBP−TRBP. To study the contribution of TRBP to siRNA asymmetry sensing in humans, we expressed and purified recombinant human TRBP as a fusion product with maltose binding protein (MBP), as well as MBP alone as a control (Figure 1). Both plasmids were generously provided by A. Gatignol (*27*, *35*). Purified MBP and MBP−TRBP products were resolved by denaturing gel electrophoresis and visualized by protein staining or Western blotting (Figure 1A−C). Proper function of the MBP−TRBP protein was then characterized by its ability to bind TAR RNA using a native gel shift assay (Figure 1D). Multiple shifted complexes were visible, consistent with the previously observed multimerization of TRBP (*35*, *36*).

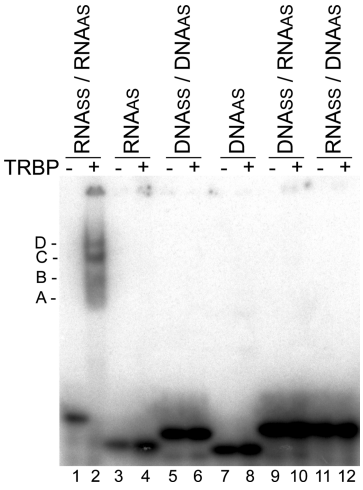

FIGURE 2: TRBP binding preferences for nucleic acids. Native gel shift assay of ^{32}P-labeled EGFP-targeting siRNA (lanes 1 and 2), ssRNA (lanes 3 and 4), siDNA (lanes 5 and 6), ssDNA (lanes 7 and 8), and DNA−RNA (lanes 9 and 10) or RNA/DNA (lanes 11 and 12) hybrids with (+) or without (−) 2000 nM MBP−TRBP. Shifted MBP−TRBP−siRNA complexes are indicated by A (approximately monomer of MBP−TRBP with siRNA), B (dimer of MBP−TRBP), C (tetramer of MBP−TRBP), and D (higher-order structure of MBP−TRBP). Note that the gel shift of the second ssRNA, RNA_{ss}, is shown in Figure 6B.

TRBP Binds dsRNA with the Greatest Affinity. TRBP has previously been shown to bind siRNAs (*37*−*39*). We also found that to be the case in a native gel shift assay (Figure 2, lanes 1 and 2) with MBP−TRBP and an siRNA targeting EGFP used previously (*40*). Nucleic acid sequence information is provided in Tables 1−5 of the Supporting Information. MBP−TRBP formed at least four distinct shifted complexes with the siRNA, corresponding approximately to complexes containing at least one siRNA molecule in a complex with one, two, four, or approximately six MBP−TRBP molecules (Figure S1 of the Supporting Information). As expected, larger complexes became more prominent at higher MBP−TRBP concentrations. Furthermore, although TRBP can bind long ssRNAs (*41*), no binding was observed for the ssRNA corresponding to the antisense (AS) (Figure 2, lanes 3 and 4) or sense (SS) (Figure 6B, EGFP S strand) strands of the duplex siRNA at this MBP−TRBP concentration. In addition, no binding was found for an siDNA or the corresponding single-stranded AS siDNA counterpart (Figure 2, lanes 5−8). We next tested DNA−RNA hybrids as these have been shown to be RNAi-competent (*37*, *42*, *43*). Somewhat surprisingly, no binding was detected with the heteroduplexes, either. Repeating the experiment with MBP alone confirmed that any observed binding was due to TRBP and not nonspecific binding by the MBP portion of the fusion product (Figure S2 of the Supporting Information). These results are consistent with TRBP requiring A-form, double-stranded RNA regions for high-affinity binding, typical of dsRBPs containing dsRBDs (*44*).

TRBP Binds Preferentially to One Strand of an Asymmetric siRNA. It has been hypothesized that TRBP senses siRNA asymmetry and therefore contributes to guide strand selection in RISC. To investigate this putative function of TRBP, we prepared three siRNAs, two of which are known to load into *Drosophila* RISC on the basis of their strand thermodynamics (*34*) and are consistent with $\Delta\Delta G$ energetics calculated with existing methods (*45*) using current nearest-neighbor parameters and a terminal A·U penalty of 0.5 kcal/mol (*46*). These

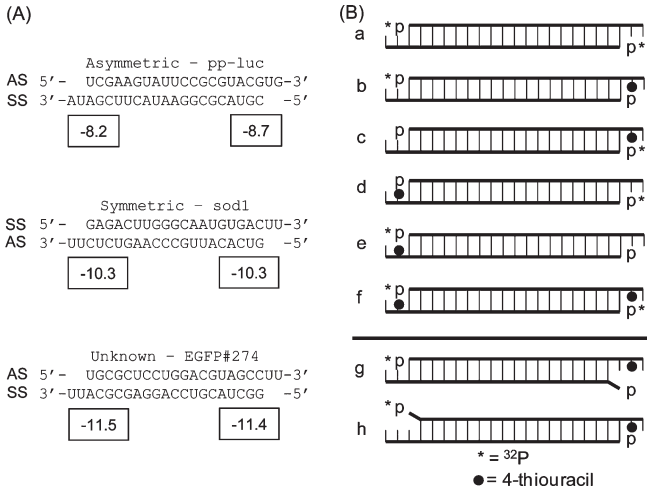

FIGURE 3: Nucleic acids used. (A) Three siRNA sequences were used in this study. Two have been documented previously for their asymmetric (pp-luc; in the text termed sequence A) or symmetric (sod1, sequence S) silencing activities and recognition by the Dicer-2−R2D2 complex in *Drosophila* (*7*, *34*). The third was previously used for EGFP silencing (EGFP, sequence G) and was expected to be slightly asymmetric on the basis of silencing activity (*40*) and $\Delta\Delta G$ calculation with mfold (*57*). AS denotes the antisense strand and SS the sense strand. Boxed numbers indicate ΔG values (in kilocalories per mole) calculated from the four terminal nearest-neighbor base pairs, including the A·U penalty and 3′-overhang contribution (single base stacking energy). (B) A series of eight different siRNAs were created for each sequence as described in the text. The strand location in panel A matches the strand location in panel B. An asterisk denotes strands 5′-labeled with [^{32}P]ATP; black circles denote 4-thiouracil modifications at position 20. siRNAs g and h contain a single 5′-terminal mismatch as indicated by the protruding base.

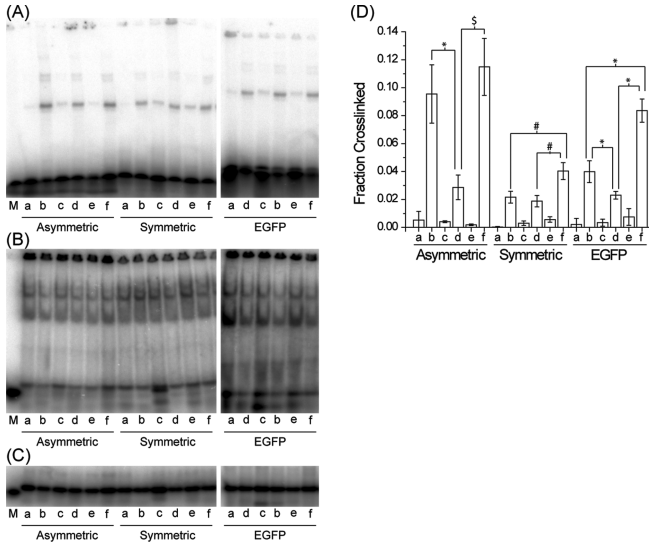

FIGURE 4: TRBP asymmetry sensing. The siRNAs in Figure 3 were tested by a gel shift assay with recombinant MBP−TRBP for (A) cross-linking, (B) native binding, or (C) native loading control, as described in the text and Materials and Methods. (D) The fraction of siRNA cross-linked by MBP−TRBP was quantified within each lane [fraction cross-linked = cross-linked signal/(cross-linked signal + un-cross-linked signal)]. Values are averages ± the standard deviation; in terms of the number of measurements (n), there were ≥5 for A and G and ≥3 for S. M denotes 21 nt single-stranded RNA used as a denaturing size marker. Note that EGFP b and d siRNAs were interchanged on the gels as compared to the asymmetric or symmetric gel loading. Symbols indicate statistically significant differences: (*) $p < 1 \times 10^{-4}$, ($) $p < 1 \times 10^{-3}$, and (#) $p < 1 \times 10^{-2}$. For complete statistical comparisons, see Table 6 of the Supporting Information.

sequences correspond to pp-luciferase (asymmetric, A; $\Delta\Delta G$ = ΔG for the AS 5′-end − ΔG for the SS 5′-end = 0.5 kcal/mol) and human Cu,Zn-superoxide dismutase (sod1) (symmetric, S; $\Delta\Delta G$ = 0.0 kcal/mol). The third sequence targets EGFP and was found to be moderately active (~60% knockdown at a concentration of 33 nM) from our previous work in human HeLa and HepG2 cells but is predicted to be essentially symmetric (EGFP, G; $\Delta\Delta G$ = −0.1 kcal/mol) (Figure 3A) (*40*). Position 20 of each strand was chemically modified with a 4-thiouracil to allow for position-specific photo-cross-linking (*47*), similar to the methods used for characterizing the *Drosophila* proteins using 5-iodoracil-modified siRNAs (*7*). For each of these sequences, a total of six different siRNAs were created by alternately hot ([γ-^{32}P]ATP) or cold (ATP) end labeling the chemically modified or unmodified single-stranded RNAs, followed by annealing with the corresponding complementary strand (Figure 3B, a−f).

The relative cross-linking efficiency of each siRNA was then determined using recombinant MBP−TRBP in a denaturing gel shift assay (Figure 4A,D). MBP−TRBP exhibited stronger cross-linking to the asymmetric b siRNA (Ab) relative to the d (Ad) structure (Figure 4A,D; compare Ab to Ad) and similarly for the EGFP siRNA (Figure 4A,D; compare Gb to Gd). However, almost equal cross-linking was detected for the symmetric siRNA Sb and Sd forms (Figure 4A,D; compare Sb to Sd). As expected, little signal was returned when the radiolabel and cross-linker were not present on the same strand, showing that cross-linking is specific for the 4-thiouracil positions (Figure 4A,D; compare b, d, and f to a, c, and e). As further confirmation, for all three siRNAs, the cross-linking of f was approximately the sum of b and d. Since all siRNAs were bound equally in a native gel shift assay (Figure 4B) and were comparably loaded (Figure 4C), we conclude that recombinant MBP−TRBP preferentially cross-links to the more stably hybridized end of the siRNA duplex. Similar trends were observed using HepG2 cytoplasmic extracts (Figure S3 of the Supporting Information), confirming that this behavior is not purely an in vitro artifact and that TRBP can detect siRNA asymmetry in the presence of other proteins, both competing and not.

It should be noted that the absolute level of cross-linking varies among the three sequences (compare the f signals for each sequence). We were unable to identify one factor that determined the overall cross-linking efficiency for a particular sequence. However, because the f signals for each sequence equal the sum of the b and d signals, comparisons within a particular duplex can be reliably made. It is tempting to attribute the differences in cross-linking to the differences in overhang sequence among the three siRNAs. However, the symmetric and EGFP sequences both have 3′-UU overhangs on each strand, with the cross-linking still asymmetric for the EGFP sequence. Thus, while other sequence or structural factors may alter the cross-linking efficiency of each siRNA relative to another siRNA, comparisons of b versus d for any single sequence reveal the presence or absence of asymmetry within a sequence and the ability of TRBP to detect the asymmetry.

Terminal Mismatches Can Weaken Binding and Cross-Linking by TRBP. Since the terminal base pairs in the siRNA have been shown to be critical for establishing siRNA asymmetry, we next considered what effect the introduction of sequence mismatches would have on TRBP asymmetry sensing (analogous to ref *7* for R2D2). Single-nucleotide mismatches were

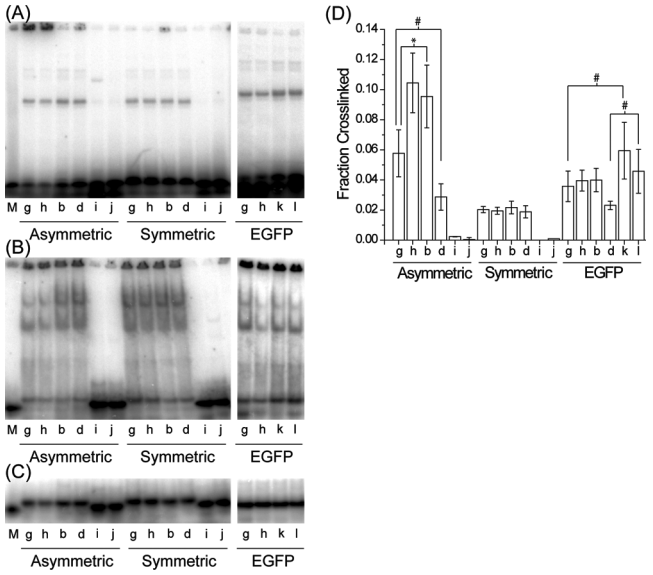

FIGURE 5: Mismatched siRNAs alter TRBP asymmetry. The siRNAs were tested via a gel shift assay for (A) cross-linking, (B) native binding, or (C) native loading control, and (D) the fraction of siRNA cross-linked by MBP−TRBP was quantified within each lane, as described in the legend of Figure 4. Values are averages ± the standard deviation; $n \geq 3$. M denotes single-stranded siRNA used as denaturing size marker. Symbols indicate statistically significant differences: (*) $p < 1 \times 10^{-2}$, and (#) $p < 3 \times 10^{-2}$. For complete statistical comparisons, see Table 6 of the Supporting Information.

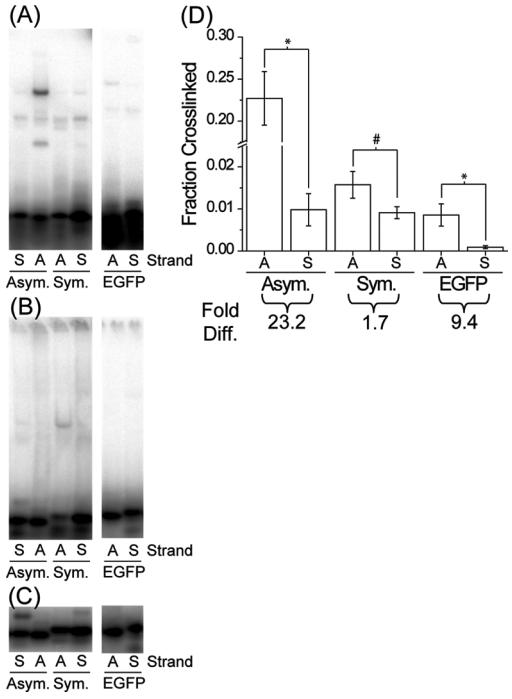

FIGURE 6: TRBP recognition of 21 nt single-stranded RNAs. The ssRNAs from each siRNA duplex were tested by a gel shift assay for (A) cross-linking, (B) native binding, or (C) native loading control, and (D) the fraction of siRNA cross-linked by MBP−TRBP was quantified within each lane, as described in the legend of Figure 4. Values are averages ± the standard deviation; $n \geq 4$. Note the break in the ordinate indicated by the cross-hatch. The Fold Diff. values listed below the graph are the ratios between the AS fraction cross-linked and the SS fraction cross-linked. Symbols indicate statistically significant differences: (*) $p < 1 \times 10^{-3}$, and (#) $p < 2 \times 10^{-2}$.

introduced at position 1 or 19 of the bottom strand of each siRNA (Figure 3; compare g and h to b). The bottom strands were cold labeled and then annealed to the hot labeled, chemically modified top strand. The mismatched ends should be destabilized, weakening TRBP binding and either reducing (g) or increasing (h) the level of cross-linking. Each siRNA was tested with recombinant MBP−TRBP in the gel shift assays (Figure 5; compare g and h to b for each siRNA). For the asymmetric sequence, a mismatch at the 5′-end of the SS did result in a reduced level of cross-linking (Figure 5A,D; compare Ag to Ab). However, we only detected a modest increase in the level of cross-linking as a result of the mismatch at the AS 5′-end (Figure 5D; compare Ah to Ab). This may reflect the fact that this asymmetric sequence already has strongly biased TRBP cross-linking, so increasing the level of asymmetry cannot further enhance binding to the more stable end. However, for the symmetric and EGFP sequences, neither mismatch resulted in any statistically significant change in cross-linking (Figure 5D; compare Sg and Sh to Sb and Gg and Gh to Gb), which may be due to the ~2-fold lower level of cross-linking compared to the asymmetric sequence despite the fact that all native binding experiments indicated nearly complete binding. Taken together, our results show that mismatches can weaken TRBP binding in the expected fashion, but additional characterization will be required to determine why this effect is not consistent for all siRNAs in our system.

TRBP Does Not Bind DNA−RNA Heteroduplexes. As we saw similar binding but different cross-linking among the three siRNAs, we wanted to revisit MBP−TRBP binding and cross-linking of DNA−RNA hybrids (Figure 5). For all three of the sequences tested, none were appreciably bound (Figure 2, lanes 9−12, where the sequences of the heteroduplexes tested, for binding only, correspond to the EGFP sequence; also Figure 5B, i and j, where i and j correspond to b and d, respectively, in Figure 3, with the bottom or top strand of the siRNAs replaced with DNA) or cross-linked by MBP−TRBP (Figure 5A,D, i and j). It has been shown recently that 5′-O-methyl modifications can alter guide strand selection and the propensity for off-target silencing (*48*), presumably by preventing 5′-phosphorylation by hClp (*49*). To examine the effect of this modification on TRBP binding and asymmetry sensing, we created EGFP siRNAs with the 5′-O-methyl modification on either end and the 4-thiouracil-modified complementary strand being radiolabeled (Gk with the bottom strand containing the 5′-O-methyl corresponds to Gg because the 5′-O-methyl groups are available only on T nucleotides and consequently introduced a C·T mismatch at that end; Gl corresponds to Gd with the top strand modified). We expected the level of binding and therefore cross-linking in both cases to decrease due to the proximity of the 5′-O-methyl group and the 4-thiouracil modification. However, the methylation had no apparent effect on MBP−TRBP binding and instead increased the overall amount of cross-linking (Figure 5A,D; compare Gk to Gg and Gl to Gd). Thus, precluding the interaction with TRBP is likely not the means by which these modifications prevent incorporation of these strands into RISC, and the cellular effects on activity or off-target silencing are a result of additional factors associated with the RLC or RISC, such as Dicer which has a lower affinity for 5′-O-methyl-modified siRNAs (*50*).

TRBP Differentially Binds Small Single-Stranded RNAs. Given that TRBP can sense siRNA asymmetry, and despite its apparent inability to effectively bind short ssRNA (Figure 2), we also wanted to consider whether any other short ssRNA sequences could be bound or cross-linked by

MBP−TRBP. We repeated the gel shift assay with the individually hot labeled, 4-thiouracil-modified ssRNAs from each of the three siRNA sequences, at an increased MBP−TRBP concentration (~3-fold higher, 1200 nM) (Figure 6). Intriguingly, the strand favorably cross-linked when part of the asymmetric siRNAs (Figure 4A,D, b for A and G) was also preferentially cross-linked here as a single strand (Figure 6A,D; compare AS to SS for A and G), whereas the single strands corresponding to the symmetric siRNA were cross-linked more evenly (Figure 6A,D; compare AS to SS for S). Curiously, the native binding pattern did not appear to reflect that of the cross-linking gel (Figure 6B), which might be expected for a relatively low-affinity interaction that could be altered by the conditions for electrophoresis, nor are the patterns a direct result of ssRNA self-dimers being recognized by TRBP (Figure 6; compare A and B to C).

As with siRNA cross-linking, the overall cross-linking efficiency among the single-stranded sequences varies (Figure 6). This further suggests that cross-linking efficiency may be affected by the sequence of the ssRNA or siRNA. Still, if each antisense strand is compared to its complementary sense strand, there is a preference toward cross-linking the antisense strand in each case, with a more pronounced preference for the ssRNAs from the siRNAs that cross-linked asymmetrically. While this supports our contention that sequence matters in TRBP−RNA interactions, further study will certainly be required to explain this result completely and to ascertain the influence of factors such as base position and 5′-end versus 3′-end effects.

DISCUSSION

Of the roles of the three proteins known to constitute the minimal human RLC, Dicer, Ago2, and TRBP, only the functional role of TRBP in the complex had not been concretely established. Here, we show for the first time that TRBP alone binds preferentially to one end of asymmetric siRNAs in vitro, presumably leading to asymmetry in the eventual guide strand loading onto Ago2. The capacity to bind both siRNAs and 21 nt ssRNAs suggests a potential role for TRBP prior to, during, and possibly after passenger strand cleavage by Ago2.

An important step in RLC formation is the initial binding of the double-stranded siRNA duplex. Dicer and Ago2 appear to be less capable of binding siRNA alone (*19*, *51*), while TRBP shows a relatively higher affinity [$K_D \sim 1-100$ nM (data not shown and ref *38*)]. When in solution, TRBP homodimerizes (*10*, *14*), which may contribute to TRBP forming multimeric complexes on dsRNA as short as 21 bp [e.g., siRNA (Figure 2 and Figure S1 of the Supporting Information)] in an uncooperative manner (*38*). This suggests that TRBP is functionally distinct from dsRBPs that show improved binding with dsRNA length, such as *Caenorhabditis elegans* RDE-4 (*38*). Consistent with what has been observed for other dsRBPs and with dsRBD function in general (*44*, *52*), TRBP was unable to bind double-stranded siDNA or RNA−DNA hybrids (Figures 2 and 5). Though some DNA substitutions are tolerated in siRNAs for gene silencing (*37*), substitutions at the 3′-end disrupted silencing, presumably by impairing TRBP binding. These results are in agreement with our observations (Figures 2 and 5), and it would be interesting to see how shorter DNA segments spread throughout the siRNA would impact binding and cross-linking by TRBP.

Though all siRNAs appear to be bound by TRBP with a similar high affinity, and apparently in a manner independent of sequence (Figures 4B and 5B and data not shown), in our hands, TRBP showed a clear asymmetry in cross-linking, seemingly driven by both sequence and strand thermodynamics (Figures 4 and 6). TRBP recognized two siRNAs asymmetrically (A and G) and one symmetrically (S) in our cross-linking gel shift assay (Figure 4A,D). For two of the siRNAs tested, our results are consistent with those previously shown in *Drosophila* RISC loading (*34*) and in cross-linking by the Dicer-2−R2D2 complex (*7*) and agree with relative thermodynamic asymmetries calculated by established techniques (*45*) (Figure 3A). Interestingly, the third sequence (G) is predicted to be only minimally asymmetric ($\Delta\Delta G = -0.1$ kcal/mol), but favoring the opposite end from what was experimentally determined (Figures 3 and 4, Gb vs Gd). Thus, published methods for calculating asymmetry do not satisfactorily predict all of our observations with recombinant MBP−TRBP.

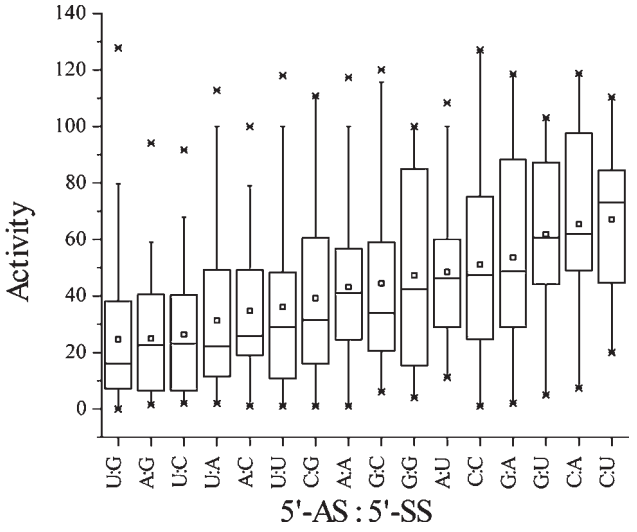

FIGURE 7: Computational analysis of first nucleotide influence on siRNA activity. siRNAs from the literature (*54*) were sorted according to the nucleotides at both the AS 5′-end and the SS 5′-end (5′-AS:5′-SS) and plotted in order of decreasing mean silencing activity. The small box indicates the mean, and the center line indicates the median. The lower and upper box lines indicate the 25th and 75th percentiles. The the outer bars indicate the 95th percentile and the points outliers.

We attempted to define other parameters that predicted all of our experimental results. We noticed that both the A and G siRNAs contained an A·U base pair at the AS 5′-end and a G·C base pair at the SS 5′-end, whereas the S siRNA contained a G·C base pair at both ends. Thus, asymmetry based solely on the first base or base pair on each end of the siRNAs would be sufficient to explain the TRBP cross-linking. A similar conclusion was reached from a computational analysis, finding that one nearest-neighbor parameter at each end of the siRNA gave the best predictive value for silencing activity (*32*). In addition, recent work shows, both in vivo and using an in vitro cross-linking assay, that the terminal sequence of miRNA and miRNA* strands results in their being preferentially loaded onto either Ago1 or Ago2 in *Drosophila* (*53*). Thus, the influence of terminal sequence appears to be a general phenomenon of the RNAi pathway.

We pursued this further through analysis of a literature data set (*54*), as we had in previous work investigating mRNA target structure effects (*40*). We sorted the tabulated siRNA activities according to the nucleotide at the 5′-end of the AS relative to the nucleotide at the 5′-end of the SS. The most active siRNAs tend

to have a U at the 5′-end of the AS and a G at the 5′-end of the SS (Figure 7 and Figure S4 of the Supporting Information). Generally, the order of nucleotide preference was U > A > G > C for the 5′-nucleotide on the AS and G > C > A > U for the 5′-nucleotide on the SS. These observations agree completely with those made earlier by Reynolds et al. (*30*). This is consistent with what would be required for thermodynamic asymmetry but also implies a role for sequence, independent of stability. For instance, a U:A combination (not base pair) is statistically more likely to be a good silencer than an A:U combination (Figure 7 and Figure S4 of the Supporting Information). While these data are for silencing efficiency, they agree with our hypothesis that asymmetry may be better predicted from only the 5′-terminal nucleotides on each siRNA strand. Further, the agreement of our analysis of this data set with our experimental findings gives us confidence that our cross-linking results are not an artifact of the three sequences chosen but a real and natural behavior of TRBP in identifying the eventual guide strand of the siRNA.

Current siRNA selection algorithms weigh duplex asymmetry heavily in choosing siRNAs likely to be highly active (*32*, *33*). While mismatches can dramatically alter relative asymmetry, our cross-linking studies did not show a consistent effect (Figure 5). In particular, for the S and G siRNAs, mismatches had no apparent effect on MBP−TRBP cross-linking, which was unexpected given that the mismatches in S were previously shown to alter its loading in *Drosophila* RISC (*7*, *34*). This may reflect a difference in the functions of the human and *Drosophila* proteins. TRBP alone may not entirely recapitulate the function of the Dicer-2−R2D2 heterodimer in *Drosophila*. Our group has recently shown that in human cytoplasmic extracts a single terminal mismatch can reduce the level of TRBP binding while enhancing Dicer binding (*55*). This suggests that, while TRBP alone can sense asymmetry in siRNAs in vitro, its sensing function in vivo may result from TRBP working in conjunction with other components of the RNAi pathway. Recent evidence further supports this coordinated function, as the termini of siRNA are predicted to be primarily occupied by Dicer and Ago2 on the basis of the structure of the human RLC (*24*).

In *Drosophila*, it was shown that the RLC (Dicer-2−R2D2−Ago2) initiates unwinding of the siRNA, with some RLCs containing ssRNAs (*7*). Our results showing TRBP cross-linking to ssRNAs (Figure 6) suggest that in humans TRBP may provide some stabilization of ssRNA-containing RLCs prior to being loaded onto Ago2. In addition, our TRBP binding results are similar to what we and others have previously found for human Dicer (*51*, *56*). Surprisingly, and potentially more importantly, TRBP preferentially cross-linked to the ssRNA known to be the guide strand in each pair (Figure 6B; compare the AS to the corresponding SS for each sequence). We examined if ssRNA secondary structure was responsible for differences in binding and cross-linking, but no patterns were discernible for structures predicted by mfold (*57*) (data not shown). We expect further investigation will reveal specific sequence or positional effects that impact TRBP−ssRNA binding and cross-linking.

While we have shown that TRBP can sense duplex asymmetry, other questions remain unanswered. Do other proteins enhance the sensing capacity of TRBP as Dicer-2 appears to in *Drosophila* (*7*)? This may be particularly important for better sensing of terminally mismatched siRNAs. Quite possibly, Dicer also assists in siRNA unwinding, perhaps through its helicase domain which has been shown to be important for processing thermodynamically unstable shRNAs (*58*). Can other proteins sense asymmetry alone? The most likely candidate is PACT, because of its known homology to TRBP and associations with Dicer, TRBP, and Ago2 (*12*, *14*, *27*). How is asymmetry best predicted? Current methods for prediction should be coupled to in vitro cross-linking and silencing readouts to assess whether factors that are important for TRBP binding in vitro are important for guide strand selection and silencing activity. Further study on this point will provide both improved siRNA activity predictions and an improved understanding of the RNAi mechanism.

ACKNOWLEDGMENT

We thank Professor Gatignol for supplying TRBP−MBP plasmids and technical advice, Professor K.-T. Jeang for supplying TAR RNA plasmids for in vitro transcription, and members of the Cellular and Biomolecular Laboratory for helpful discussions.

SUPPORTING INFORMATION AVAILABLE

siRNA sequence information and additional binding and statistical results. This material is available free of charge via the Internet at http://pubs.acs.org.

REFERENCES

1. Fire, A., Xu, S., Montgomery, M. K., Kostas, S. A., Driver, S. E., and Mello, C. C. (1998) Potent and specific genetic interference by double-stranded RNA in *Caenorhabditis elegans*. *Nature 391*, 806–811.
2. Hannon, G. J. (2002) RNA interference. *Nature 418*, 244–251.
3. Bernstein, E., Caudy, A. A., Hammond, S. M., and Hannon, G. J. (2001) Role for a bidentate ribonuclease in the initiation step of RNA interference. *Nature 409*, 363–366.
4. Elbashir, S. M., Harborth, J., Lendeckel, W., Yalcin, A., Weber, K., and Tuschl, T. (2001) Duplexes of 21-nucleotide RNAs mediate RNA interference in cultured mammalian cells. *Nature 411*, 494–498.
5. Elbashir, S. M., Lendeckel, W., and Tuschl, T. (2001) RNA interference is mediated by 21- and 22-nucleotide RNAs. *Genes Dev. 15*, 188–200.
6. Maniataki, E., and Mourelatos, Z. (2005) A human, ATP-independent, RISC assembly machine fueled by pre-miRNA. *Genes Dev. 19*, 2979–2990.
7. Tomari, Y., Matranga, C., Haley, B., Martinez, N., and Zamore, P. D. (2004) A protein sensor for siRNA asymmetry. *Science 306*, 1377–1380.
8. Chendrimada, T. P., Gregory, R. I., Kumaraswamy, E., Norman, J., Cooch, N., Nishikura, K., and Shiekhattar, R. (2005) TRBP recruits the Dicer complex to Ago2 for microRNA processing and gene silencing. *Nature 436*, 740–744.
9. Haase, A. D., Jaskiewicz, L., Zhang, H., Laine, S., Sack, R., Gatignol, A., and Filipowicz, W. (2005) TRBP, a regulator of cellular PKR and HIV-1 virus expression, interacts with Dicer and functions in RNA silencing. *EMBO Rep. 6*, 961–967.
10. MacRae, I. J., Ma, E., Zhou, M., Robinson, C. V., and Doudna, J. A. (2008) In vitro reconstitution of the human RISC-loading complex. *Proc. Natl. Acad. Sci. U.S.A. 105*, 512–517.
11. Robb, G. B., and Rana, T. M. (2007) RNA Helicase A Interacts with RISC in Human Cells and Functions in RISC Loading. *Mol. Cell 26*, 523–537.
12. Lee, Y., Hur, I., Park, S. Y., Kim, Y. K., Suh, M. R., and Kim, V. N. (2006) The role of PACT in the RNA silencing pathway. *EMBO J. 25*, 522–532.
13. Gregory, R. I., Chendrimada, T. P., Cooch, N., and Shiekhattar, R. (2005) Human RISC Couples MicroRNA Biogenesis and Posttranscriptional Gene Silencing. *Cell 123*, 631–640.
14. Kok, K. H., Ng, M. H., Ching, Y. P., and Jin, D. Y. (2007) Human TRBP and PACT Directly Interact with Each Other and Associate with Dicer to Facilitate the Production of Small Interfering RNA. *J. Biol. Chem. 282*, 17649–17657.
15. Liu, J., Carmell, M. A., Rivas, F. V., Marsden, C. G., Thomson, J. M., Song, J. J., Hammond, S. M., Joshua-Tor, L., and Hannon, G. J. (2004) Argonaute2 Is the Catalytic Engine of Mammalian RNAi. *Science 305*, 1437–1441.

16. Meister, G., Landthaler, M., Patkaniowska, A., Dorsett, Y., Teng, G., and Tuschl, T. (2004) Human Argonaute2 Mediates RNA Cleavage Targeted by miRNAs and siRNAs. *Mol. Cell 15*, 185–197.
17. Rand, T. A., Petersen, S., Du, F., and Wang, X. (2005) Argonaute2 Cleaves the Anti-Guide Strand of siRNA during RISC Activation. *Cell 123*, 621–629.
18. Song, J. J., Smith, S. K., Hannon, G. J., and Joshua-Tor, L. (2004) Crystal Structure of Argonaute and Its Implications for RISC Slicer Activity. *Science 305*, 1434–1437.
19. Rivas, F. V., Tolia, N. H., Song, J. J., Aragon, J. P., Liu, J., Hannon, G. J., and Joshua-Tor, L. (2005) Purified Argonaute2 and an siRNA form recombinant human RISC. *Nat. Struct. Mol. Biol. 12*, 340–349.
20. Matranga, C., Tomari, Y., Shin, C., Bartel, D. P., and Zamore, P. D. (2005) Passenger-Strand Cleavage Facilitates Assembly of siRNA into Ago2-Containing RNAi Enzyme Complexes. *Cell 123*, 607–620.
21. Kim, D. H., Behlke, M. A., Rose, S. D., Chang, M. S., Choi, S., and Rossi, J. J. (2005) Synthetic dsRNA Dicer substrates enhance RNAi potency and efficacy. *Nat. Biotechnol. 23*, 222–226.
22. Siolas, D., Lerner, C., Burchard, J., Ge, W., Linsley, P. S., Paddison, P. J., Hannon, G. J., and Cleary, M. A. (2005) Synthetic shRNAs as potent RNAi triggers. *Nat. Biotechnol. 23*, 227–231.
23. Rose, S. D., Kim, D. H., Amarzguioui, M., Heidel, J. D., Collingwood, M. A., Davis, M. E., Rossi, J. J., and Behlke, M. A. (2005) Functional polarity is introduced by Dicer processing of short substrate RNAs. *Nucleic Acids Res. 33*, 4140–4156.
24. Wang, H. W., Noland, C., Siridechadilok, B., Taylor, D. W., Ma, E., Felderer, K., Doudna, J. A., and Nogales, E. (2009) Structural insights into RNA processing by the human RISC-loading complex. *Nat. Struct. Mol. Biol. 16*, 1148–1153.
25. Gatignol, A., Buckler-White, A., Berkhout, B., and Jeang, K. T. (1991) Characterization of a human TAR RNA-binding protein that activates the HIV-1 LTR. *Science 251*, 1597–1600.
26. Benkirane, M., Neuveut, C., Chun, R. F., Smith, S. M., Samuel, C. E., Gatignol, A., and Jeang, K. T. (1997) Oncogenic potential of TAR RNA binding protein TRBP and its regulatory interaction with RNA-dependent protein kinase PKR. *EMBO J. 16*, 611–624.
27. Laraki, G., Clerzius, G., Daher, A., Melendez-Pena, C., Daniels, S., and Gatignol, A. (2008) Interactions between the double-stranded RNA-binding proteins TRBP and PACT define the Medipal domain that mediates protein-protein interactions. *RNA Biol. 5*, 92–103.
28. Daniels, S. M., Melendez-Pena, C. E., Scarborough, R. J., Daher, A., Christensen, H. S., El Far, M., Purcell, D. F., Laine, S., and Gatignol, A. (2009) Characterization of the TRBP domain required for dicer interaction and function in RNA interference. *BMC Mol. Biol. 10*, 38.
29. Liu, Q., Rand, T. A., Kalidas, S., Du, F., Kim, H. E., Smith, D. P., and Wang, X. (2003) R2D2, a bridge between the initiation and effector steps of the *Drosophila* RNAi pathway. *Science 301*, 1921–1925.
30. Reynolds, A., Leake, D., Boese, Q., Scaringe, S., Marshall, W. S., and Khvorova, A. (2004) Rational siRNA design for RNA interference. *Nat. Biotechnol. 22*, 326–330.
31. Khvorova, A., Reynolds, A., and Jayasena, S. D. (2003) Functional siRNAs and miRNAs exhibit strand bias. *Cell 115*, 209–216.
32. Lu, Z. J., and Mathews, D. H. (2007) Efficient siRNA selection using hybridization thermodynamics. *Nucleic Acids Res. 36*, 640–647.
33. Shao, Y., Chan, C. Y., Maliyekkel, A., Lawrence, C. E., Roninson, I. B., and Ding, Y. (2007) Effect of target secondary structure on RNAi efficiency. *RNA 13*, 1631–1640.
34. Schwarz, D. S., Hutvagner, G., Du, T., Xu, Z., Aronin, N., and Zamore, P. D. (2003) Asymmetry in the assembly of the RNAi enzyme complex. *Cell 115*, 199–208.
35. Daviet, L., Erard, M., Dorin, D., Duarte, M., Vaquero, C., and Gatignol, A. (2000) Analysis of a binding difference between the two dsRNA-binding domains in TRBP reveals the modular function of a KR-helix motif. *Eur. J. Biochem. 267*, 2419–2431.
36. Cosentino, G. P., Venkatesan, S., Serluca, F. C., Green, S. R., Mathews, M. B., and Sonenberg, N. (1995) Double-stranded-RNA-dependent protein kinase and TAR RNA-binding protein form homo- and heterodimers in vivo. *Proc. Natl. Acad. Sci. U.S.A. 92*, 9445–9449.
37. Ui-Tei, K., Naito, Y., Zenno, S., Nishi, K., Yamato, K., Takahashi, F., Juni, A., and Saigo, K. (2008) Functional dissection of siRNA sequence by systematic DNA substitution: Modified siRNA with a DNA seed arm is a powerful tool for mammalian gene silencing with significantly reduced off-target effect. *Nucleic Acids Res. 36*, 2136–2151.
38. Parker, G. S., Maity, T. S., and Bass, B. L. (2008) dsRNA binding properties of RDE-4 and TRBP reflect their distinct roles in RNAi. *J. Mol. Biol. 384*, 967–979.
39. Katoh, T., and Suzuki, T. (2007) Specific residues at every third position of siRNA shape its efficient RNAi activity. *Nucleic Acids Res. 35*, e27.
40. Gredell, J. A., Berger, A. K., and Walton, S. P. (2008) Impact of target mRNA structure on siRNA silencing efficiency: A large-scale study. *Biotechnol. Bioeng. 100*, 744–755.
41. Gatignol, A., Buckler, C., and Jeang, K. T. (1993) Relatedness of an RNA-binding motif in human immunodeficiency virus type 1 TAR RNA-binding protein TRBP to human P1/dsI kinase and *Drosophila staufen*. *Mol. Cell. Biol. 13*, 2193–2202.
42. Lamberton, J. S., and Christian, A. T. (2003) Varying the nucleic acid composition of siRNA molecules dramatically varies the duration and degree of gene silencing. *Mol. Biotechnol. 24*, 111–120.
43. Hohjoh, H. (2002) RNA interference (RNA(i)) induction with various types of synthetic oligonucleotide duplexes in cultured human cells. *FEBS Lett. 521*, 195–199.
44. Saunders, L. R., and Barber, G. N. (2003) The dsRNA binding protein family: Critical roles, diverse cellular functions. *FASEB J. 17*, 961–983.
45. Hutvagner, G. (2005) Small RNA asymmetry in RNAi: Function in RISC assembly and gene regulation. *FEBS Lett. 579*, 5850–5857.
46. Mathews, D. H., Sabina, J., Zuker, M., and Turner, D. H. (1999) Expanded sequence dependence of thermodynamic parameters improves prediction of RNA secondary structure. *J. Mol. Biol. 288*, 911–940.
47. Sontheimer, E. J. (1994) Site-specific RNA crosslinking with 4-thiouridine. *Mol. Biol. Rep. 20*, 35–44.
48. Chen, P. Y., Weinmann, L., Gaidatzis, D., Pei, Y., Zavolan, M., Tuschl, T., and Meister, G. (2008) Strand-specific 5′-O-methylation of siRNA duplexes controls guide strand selection and targeting specificity. *RNA 14*, 263–274.
49. Weitzer, S., and Martinez, J. (2007) The human RNA kinase hClp1 is active on 3′ transfer RNA exons and short interfering RNAs. *Nature 447*, 222–226.
50. Pellino, J. L., Jaskiewicz, L., Filipowicz, W., and Sontheimer, E. J. (2005) ATP modulates siRNA interactions with an endogenous human Dicer complex. *RNA 11*, 1719–1724.
51. Kini, H. K., and Walton, S. P. (2007) In vitro binding of single-stranded RNA by human Dicer. *FEBS Lett. 581*, 5611–5616.
52. Bevilacqua, P. C., and Cech, T. R. (1996) Minor-groove recognition of double-stranded RNA by the double-stranded RNA-binding domain from the RNA-activated protein kinase PKR. *Biochemistry 35*, 9983–9994.
53. Ghildiyal, M., Xu, J., Seitz, H., Weng, Z., and Zamore, P. D. (2010) Sorting of *Drosophila* small silencing RNAs partitions microRNA* strands into the RNA interference pathway. *RNA 16*, 43–56.
54. Shabalina, S. A., Spiridonov, A. N., and Ogurtsov, A. Y. (2006) Computational models with thermodynamic and composition features improve siRNA design. *BMC Bioinf. 7*, 65.
55. Kini, H. K., and Walton, S. P. (2009) Effect of siRNA terminal mismatches on TRBP and Dicer binding and silencing efficacy. *FEBS J. 276*, 6576–6585.
56. Lima, W. F., Murray, H., Nichols, J. G., Wu, H., Sun, H., Prakash, T. P., Berdeja, A. R., Gaus, H. J., and Crooke, S. T. (2009) Human Dicer Binds Short Single-strand and Double-strand RNA with High Affinity and Interacts with Different Regions of the Nucleic Acids. *J. Biol. Chem. 284*, 2535–2548.
57. Zuker, M. (2003) Mfold web server for nucleic acid folding and hybridization prediction. *Nucleic Acids Res. 31*, 3406–3415.
58. Soifer, H. S., Sano, M., Sakurai, K., Chomchan, P., Saetrom, P., Sherman, M. A., Collingwood, M. A., Behlke, M. A., and Rossi, J. J. (2008) A role for the Dicer helicase domain in the processing of thermodynamically unstable hairpin RNAs. *Nucleic Acids Res. 36*, 6511–6522.